ROZPRAWY INŻYNIERSKIE • ENGINEERING TRANSACTIONS • 29, 1, 69—81, 1981
Polska Akademia Nauk • Instytut Podstawowych Problemów Techniki

CORRELATION BETWEEN STATIC AND DYNAMIC COLLAPSE OF COMPRESSED THIN-WALLED TUBES

C. MOLNAR (BUDAPEST)

Static and dynamic crush tests on a thin-walled prismatic column are described taking into account imperfections. The crushing process is regarded as a stochastic one and the results of measurements are reduced using the probability methods. Three different definitions of the mean dynamic crushing force are discussed and only one of these is shown to yield simple and reliable results. The correlation between the static and dynamic crushing force is also presented. The results obtained may be used in designing energy-absorbing supporting structures for bus safety bumpers.

1. Introduction

For designing safety bumpers to be installed on buses, the behaviour of an underframe structure stiffness should be well understood under static and dynamic loading conditions. This structure provides adequate support for energy absorbing devices. Besides, its strength determines the maximum deceleration occurring during an impact that should not be in excess of the limit value corresponding to the passengers' tolerance.

An important problem of passive safety investigations is the relation between static and dynamic tests, i.e. the correlation between static and dynamic load-carrying capacities of underframe structures.

Instead of an underframe structure of a bus, a more simple "structure" and loading technique will be analysed. In particular, the static and dynamic load-carrying capacities of square section tubes, constituting an integral (self-carrying) bus body structure, will be investigated at axial loads and the correlation between maximum and average crushing forces will be studied.

2. Various forms of losing stability by square section tubes

A typical load-compression diagram of a tube is presented in Fig. 1. Its stability and maximum load denoted by the point A are designated as the load-carrying capacity of the tube. This definition applies to both static and dynamic loading conditions.

The tube load-carrying capacity under static load is illustrated in Fig. 2 as a function of the tube length. The curve was determined on the basis of proper mechanical models; the points correspond to experimental results.

If the tube length is larger than L_2, then there will be a loss of stability in the elastic range.

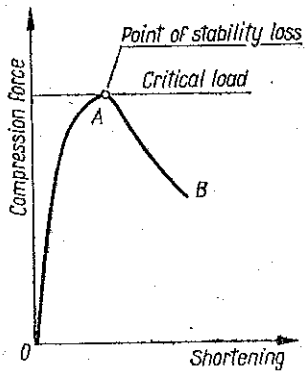

FIG. 1.

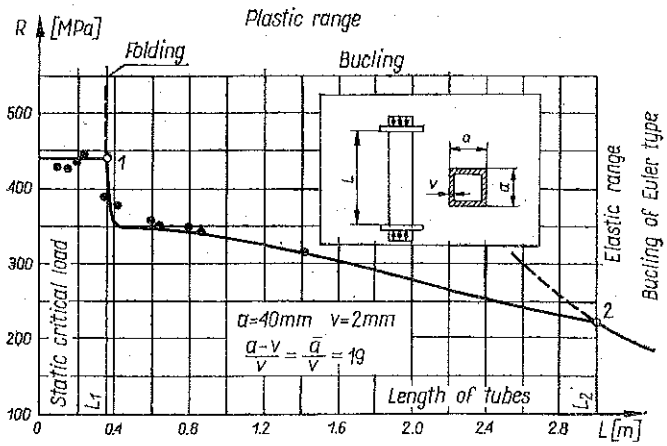

FIG. 2.

If the tube length is smaller than L_2 but larger than L_1, there will be a loss of stability in the plastic deformation range.

If the tube length is smaller than L_1, local buckling will be observed, in which regular folds are formed.

This form of the loss of stability will be dealt with in this paper. The critical length L_1 depends on the cross-section dimensions.

3. TEST FACILITIES AND MEASURING TECHNIQUES

All tests reported here were carried out on tubes having identical cross-sectional dimensions of $40 \times 40 \times 2$ mm.

Static tests were run on a conventional testing machine and load-compression diagrams were recorded on a $X-Y$ plotter. Dynamic tests were performed with several values of impact energy, impact velocity and mass of impacting weight. During our experiments three impacting weights were applied having M_T=300 kg, 600 kg and 1.000 kg respectively.

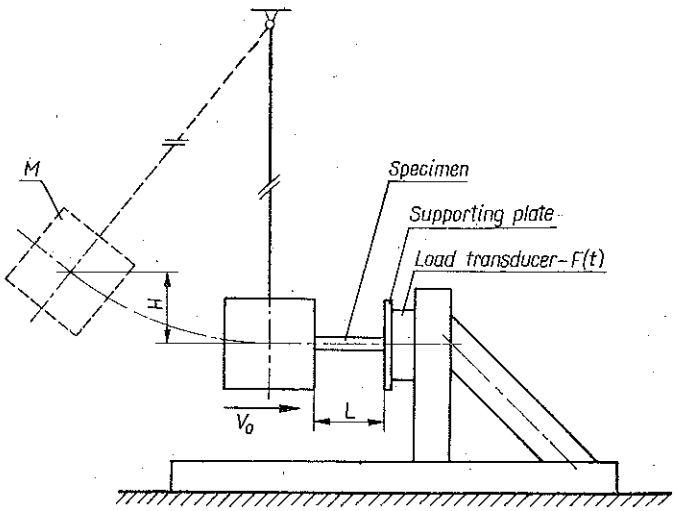

FIG. 3.

The stand for dynamic investigations is schematically illustrated in Fig. 3. Tubes with different lenghts were used, all clamped over 30 mm of its length.

The load-time history was recorded and permanent deformation of the tubes was measured.

The strength characteristics of the tubes depends strongly on geometrical, structural and material imperfections. In order to account for these effects, the measurements data are processed by using probability methods, i.e. the crushing process is regarded as a stochastic one and the quantities characterizing this are treated as random variables. For this purpose some experimental "levels" were repeated several times and data received were evaluated in the way referred to above.

4. MEAN STATIC CRUSHING FORCE

The force level is called the energy density function, Fig. 4. The critical load s denoted by F^s and the mean crushing load is defined by

$$F_m^s = \frac{1}{\delta}\int_0^{\delta} w(s)\,ds, \tag{4.1}$$

where δ is the maximum shortening of the tube. The energy absorbed by thetubec during the process of compression is shown by the shadowed area. Distribution fucnitions of critical and average loads were plotted for the specimens' (see Fig. 5) data

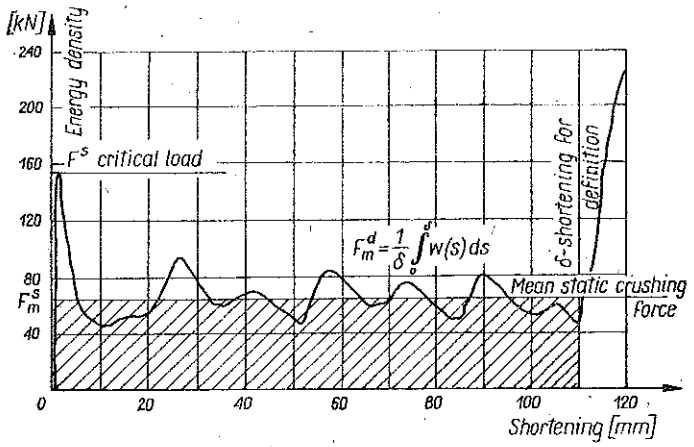
[kN]
Energy density
240
200
160
120
80
40
F^s critical load
F_m^s
$F_m^d = \frac{1}{\delta}\int_0^{\delta} w(s)\,ds$
δ-shortening for definition
Mean static crushing force
0
20
40
60
80
100
120
Shortening [mm]

FIG. 4.

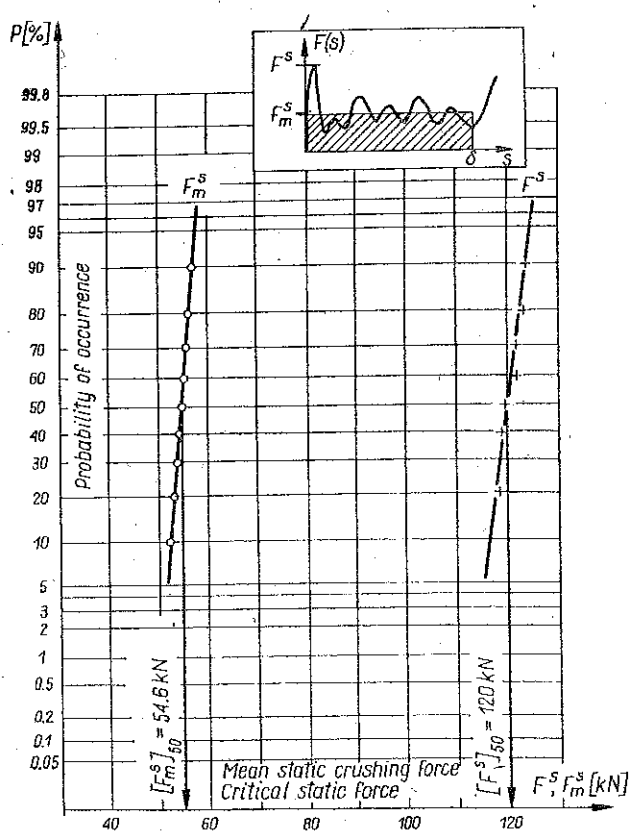
P[%]
99.8
99.5
99
98
97
95
90
80
70
60
50
40
30
20
10
5
3
2
1
0.5
0.2
0.1
0.05
Probability of occurrence
F(s)
F^s
F_m^s
δ
s
F_m^s
F^s
$[F_m^s]_{50}$ = 54.6 kN
$[F^s]_{50}$ = 120 kN
Mean static crushing force
Critical static force
F^s, F_m^s [kN]
40
60
80
100
120

FIG. 5.

assuming that the random variables follow the Gaussian distribution law. This assumption has already proved adequate during the investigations of the energy density-function characteristics. From the diagram it is possible to read the magnitudes of F_s and F_m^s corresponding to 50 per cent probability

$$[F_s]_{50}=120 \text{ kN},$$
$$[F_m^s]_{50}=54.6 \text{ kN}.$$

5. Mean crushing force during dynamic loads

A typical load-time history is shown in Fig. 6. The maximum dynamic load is denoted by F^d.

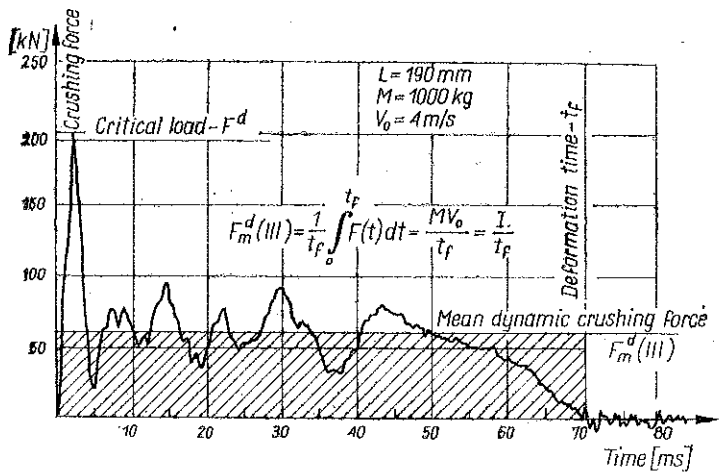

FIG. 6.

The dependence of F^d on impact velocity for various impacting masses is shown in Fig. 7, while Fig. 8 shows the variation of F^d with the impacting mass at different impact velocities. From the above diagrams it is clear that the dynamic buckling load increases with the value of the impacting mass and impact velocity. It is interesting to observe that the function F^d, when plotted against the impact energy, exhibits the straight line behaviour (Fig. 9).

In the case of dynamic loading three alternative definitions of the mean dynamic load can be given.

Depending upon whether the averaging is with respect to distance, velocity or time coordinate, respectively:

$$F_m^d(\text{I})=\frac{1}{\delta}\int_0^{\delta}F_\delta(\delta')\,d\delta', \tag{5.1}$$

$$F_m^d(\text{II})=-\frac{1}{V_0}\int_0^{V_0}F_v(V)\,dV, \tag{5.2}$$

$$F_m^d(\text{III})=\frac{1}{t_f}\int_0^{t_f}F(t)\,dt, \tag{5.3}$$

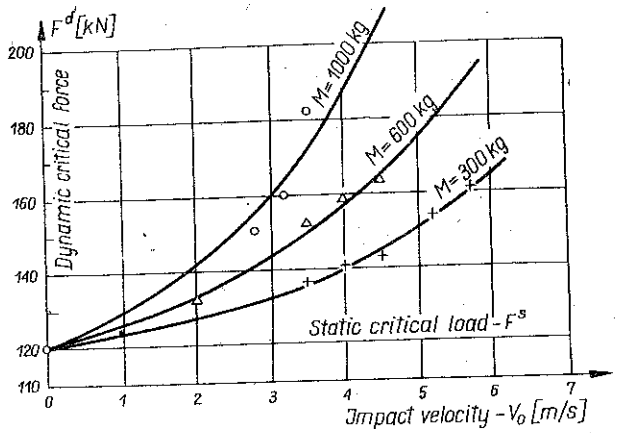

FIG. 7.

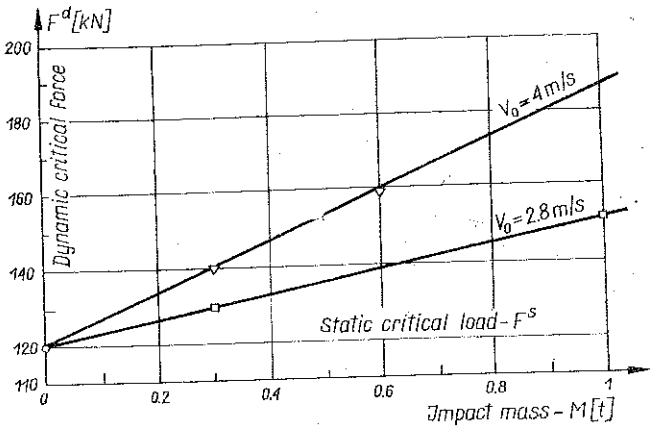

FIG. 8.

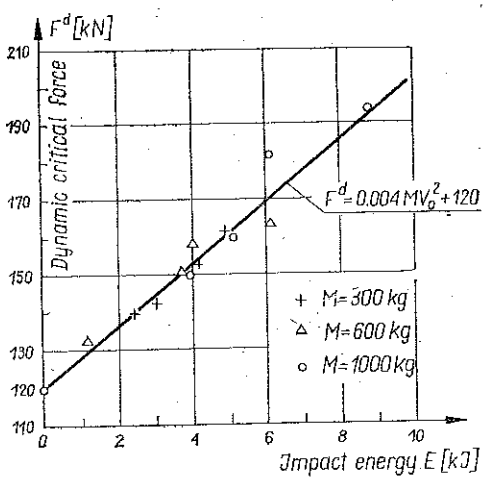

FIG. 9.

where $F(t)$ is load-time function registered during the test, V_0 — impact velocity, δ — maximum compression of the tube and t_f — duration of impact.

Assuming that the tube mass in comparison to the impacting mass may be neglected and also that tube support is perfectly rigid, accelerations, velocities and displacements of the tube end are related to the measured function $F(t)$ by

$$a(t)=\frac{F(t)}{M}, \tag{5.4}$$

$$V(t)=\frac{1}{M}\int_0^t F(\tau)\,d\tau+V_0, \tag{5.5}$$

$$\delta(t)=\frac{1}{M}\int_0^t\left[\int_0^\tau [F(t')\,dt']\right]d\tau+V_0\,t. \tag{5.6}$$

In particular, maximum deformation and impact duration may be determined from

$$\delta=-\frac{1}{M}\int_0^{t_f}\left[\int_0^t F(\tau)\,d\tau\right]dt+V_0\,t_f, \tag{5.7}$$

$$MV_0=-\int_0^{t_f} F(t)\,dt. \tag{5.8}$$

Making use of Eqs. (5.4)-(5.8), all definitions may be expressed entirely in terms of the function $F(t)$:

$$\begin{aligned} F_m^d(\mathrm{I})&=\frac{1}{\delta}\int_0^{t_f} F(t)\left[\frac{1}{M}\int_0^t F(\tau)\,d\tau+V_0\right]dt,\\ F_m^d(\mathrm{II})&=-\frac{1}{MV_0}\int_0^{t_f} F^2(t)\,dt. \end{aligned} \tag{5.9}$$

The definitions I and III may be considerably simplified:

$$F_m^d(\mathrm{I})=-\frac{\frac{1}{2}MV_0^2}{\delta}, \tag{5.10}$$

$$F_m^d(\mathrm{III})=-\frac{MV_0}{t_f}. \tag{5.11}$$

On the basis of the above relationships and using the registered signal $F(t)$, average or mean loads may be determined according to each definition. The integrations were performed using an analogue computer, Figs. 10 and 11.

It was found that permanent deformation of the tube obtained through double integration of the function $F(t)$ agrees with the independently measured permanent shortening δ (Fig. 10), which provides a check for the correctness of the force recording method.

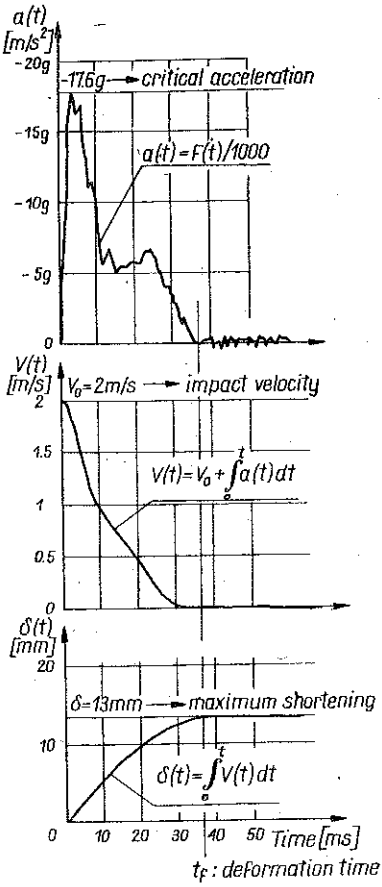
a(t) [m/s²]
-20g
-17.6g → critical acceleration
-15g
a(t)=F(t)/1000
-10g
-5g
0
V(t) [m/s]
2
V₀=2m/s → impact velocity
1.5
V(t)=V₀+∫₀ᵗ a(t)dt
1
0.5
0
δ(t) [mm]
20
δ=13mm → maximum shortening
10
δ(t)=∫₀ᵗ V(t)dt
0
10
20
30
40
50
Time [ms]
t_f : deformation time
Impact mass : 1000 kg
Impact velocity : 2 m/s
Impact energy : 2 kJ
Acceleration - time diagram
Velocity - time diagram
Shortening - time diagram

FIG. 10.

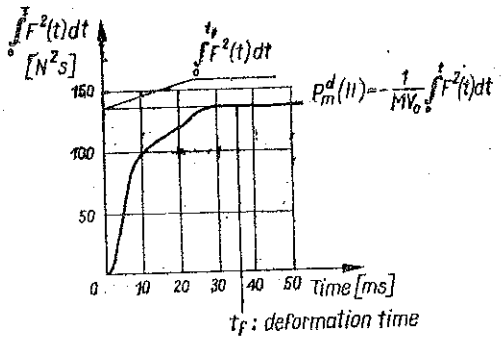
∫₀ᵀ F²(t)dt
[N²s]
∫₀^{t_f} F²(t)dt
P_m^d(II)=-1/MV₀ ∫₀^{t_f} F²(t)dt
150
100
50
0
10
20
30
40
50
Time [ms]
t_f : deformation time

FIG. 11.

The average compressing load, computed on the basis of definition I, versus the impact velocity at various impacting masses is shown in Fig. 12. The maximum observed on the curves is due to a larger contribution of the first folding. The explanation of the observed maximum is that during impacts at low velocity only one or two folds are produced on the tube and the contribution of the first fold which requires higher energy is more pronounced.

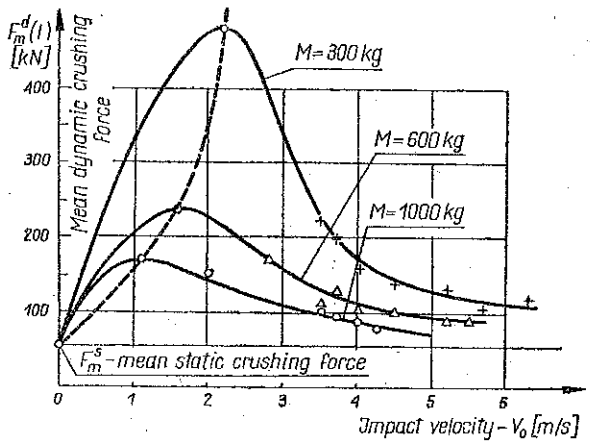

FIG. 12.

In Fig. 13 the average load is illustrated as a function of impacting mass with impact velocity as a parameter.

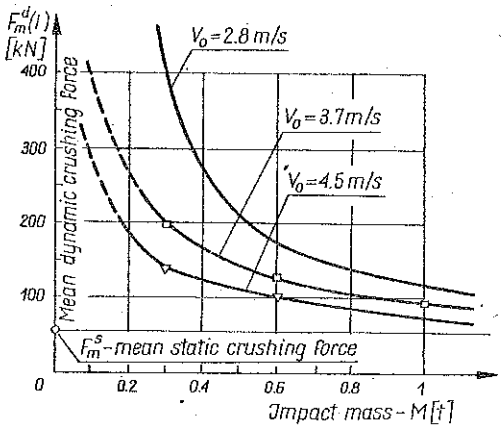

FIG. 13

In Fig. 14 the average compression load determined on the basis of definition II is illustrated as a function of impact velocity.

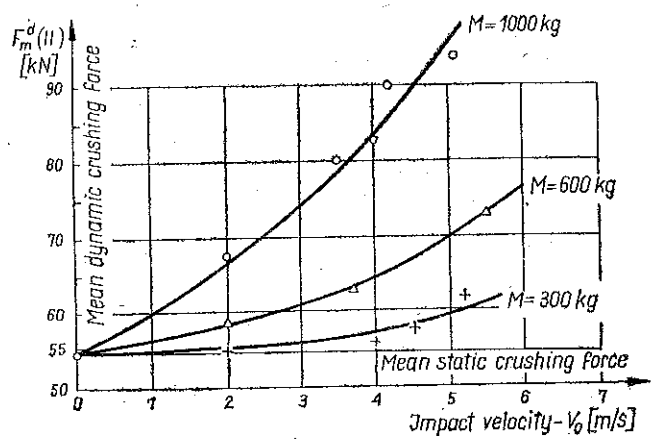

FIG. 14.

The results obtained on the basis of definition III are shown in Fig. 15. The trend of experimental points suggests that the average compression load value depends linearly on the impact velocity and is independent of the impacting mass.

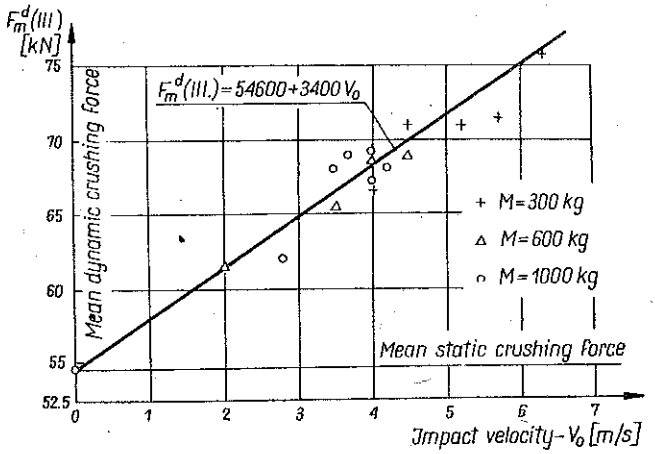

FIG. 15.

A comparison of the results obtained by means of all three definitions for the case of impacting mass $M=1.000$ kg are shown in Fig. 16.

Differences in the predicted mean compressive force are seen to be appreciable.

The performed analysis shows that definition III seems to be the simplest one as it is dependent only on impact velocity value, and may easily be calculated once t_f is read off from the load-time diagram $F(t)$.

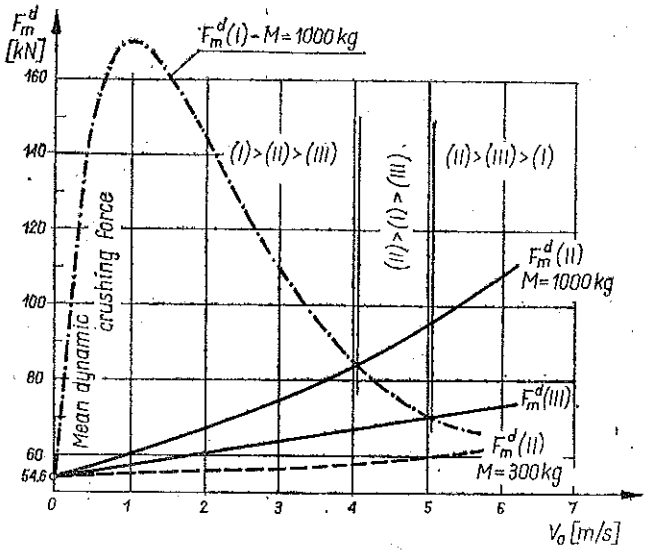

FIG. 16.

6. CORRELATION BETWEEN STATIC AND DYNAMIC LOADS

From the results obtained so far, the ratio of static to dynamic loads (critical and average compression loads) might easily be calculated.

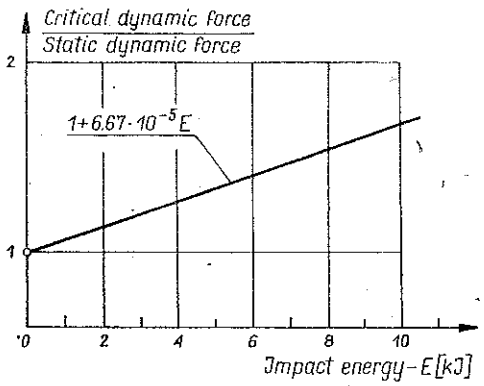

FIG. 17.

This ratio called the correction factor is plotted in Fig. 17 as a function of impact energy, while the dependence of dynamic correction factor on the impact velocity is illustrated in Fig. 18. In the latter figure the literature data are also given showing a good agreement with our curves.

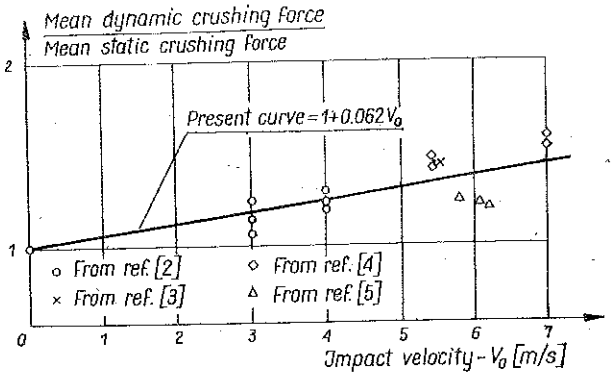

FIG. 18.

7. CONCLUSIONS

In the case of thin-walled tubes of rectangular cross-section the dependence of the critical load and the average compression load on impact parameters was investigated under axial compression.

A correlation between static and dynamic experiments has clearly been demonstrated. The obtained results might be used for verifying energy absorbing capabilities of structures which provide support to bus safety bumpers. Such studies in view of the high costs of passive safety experiments, appear to be necessary.

REFERENCES

1. T. AKERSTRÖM, T. WIERZBICKI, *Dynamic crushing of strain rate sensitive box columns*, Second International Conference of Vehicle Structural Mechanics, Michigan Inn, Southfield, Michigan, April 18–20, 1977.
2. Y. OHKUBO, T. AHAMATSU, K. SHIRASAWA, *Meane crushing strength of closed-hat section members*, SAE Paper 740040.
3. A. WIMMER, *Einfluss der Belastungsgeschwindigkeit auf das Festigkeits und Verformungsverhalten von Blechkonstruktionen am Beispiel von Kraft-fahrzeugen*, ATZ, 77, 10, pp. 281–286, 1975.
4. M. SHIBUSAWA, T. TAKANO, S. OSHITA, *Buckling behaviour of members of vehicle structure*, J.S.A.E Japan, 27, 5, pp 510–519, 1973.
5. M. YAMAYA, M. TANI, *Energy absorption by the plastic deformation of sheet metal columns with box-shaped cross section*, Mits. Techn. Rev., 8, pp. 59–66, 1971.

STRESZCZENIE

PORÓWNANIE STATYCZNEJ I DYNAMICZNEJ WYTRZYMAŁOŚCI NA ZGNIATANIE CIENKOŚCIENNYCH KOLUMN

Opisany jest program doświadczeń dotyczący statystycznego i dynamicznego obciążenia pryzmatycznych kolumn pozwalający na zbadanie efektu imperfekcji. Traktując proces zguiatania jako proces stochastyczny, wyniki pomiarów opracowane zostały przy wykorzystaniu metod

probabilistycznych. Podane są trzy różne definicje średniej dynamicznej siły ściskającej i wskazane jest, że tylko jedna z nich prowadzi do wiarygodnych, a jednocześnie prostych wyników. Przedstawiono korelację pomiędzy statyczną i dynamiczną siłą ściskającą. Uzyskane wyniki mogą zostać wykorzystane przy projektowaniu konstrukcji bezpiecznego zderzaka autobosu.

Резюме

СРАВНЕНИЕ СТАТИЧЕСКОЙ И ДИНАМИЧЕСКОЙ ПРОЧНОСТИ НА СДАВЛЕНИЕ ТОНКОСТЕННЫХ КОЛОНН

Описана программа экспериментов касающаяся статического и динамического нагружений призматических колонн позволяющая исследовать эффект имперфекции. Трактуя процесс сдавления как стохастический процесс, результаты измерений разботаны при использовании пробабилистических методов. Приведены три разные определения средней динамической сжимающей силы и указано на то, что только одно из них приводит к достоверным, и одновременно простым результатам. Представлена корреляция между статической и динамической сжимающими силами. Полученные результаты могут быть использованы при проектировании конструкции безопасного буфера автобуса.

RESEARCH INSTITUTE OF AUTOMOTIVE INDUSTRY, BUDAPEST, HUNGARY

Received February 15, 1980.